



1 **Assessing the impact of anthropogenic pollution on isoprene-derived secondary organic**
2 **aerosol formation in PM_{2.5} collected from the Birmingham, Alabama ground site during the**
3 **2013 Southern Oxidant and Aerosol Study**

4

5 W. Rattanavaraha¹, K. Chu¹, S. H. Budisulistiorini^{1,a}, M. Riva¹, Y.-H. Lin^{1,b}, E. S. Edgerton², K.
6 Baumann², S. L. Shaw³, H. Guo⁴, L. King⁴, R. J. Weber⁴, E. A. Stone⁵, M. E. Neff⁵, J. H.
7 Offenberg⁶, Z. Zhang¹, A. Gold¹, and J. D. Surratt^{1,*}

8

9 ¹ Department of Environmental Sciences and Engineering, Gillings School of Global Public
10 Health, The University of North Carolina at Chapel Hill, Chapel Hill, NC, USA

11 ² Atmospheric Research & Analysis, Inc., Cary, NC, USA

12 ³ Electric Power Research Institute, Palo Alto, CA, USA

13 ⁴ Earth and Atmospheric Science, Georgia Institute of Technology, Atlanta, GA, USA

14 ⁵ Department of Chemistry, University of Iowa, Iowa City, IA, USA

15 ⁶ Human Exposure and Atmospheric Sciences Division, United States Environmental Protection
16 Agency, Research Triangle Park, NC, USA

17 ^a now at: Earth Observatory of Singapore, Nanyang Technological University, Singapore

18 ^b now at: Michigan Society of Fellows, Department of Chemistry, University of Michigan, Ann
19 Arbor, MI, USA

20

21 * To whom correspondence should be addressed. Email: surratt@unc.edu

22 For Submission to: Atmospheric Chemistry & Physics Discussions

23



24 Abstract

25 In the southeastern U.S., substantial emissions of isoprene from deciduous trees undergo
26 atmospheric oxidation to form secondary organic aerosol (SOA) that contributes to fine particulate
27 matter (PM_{2.5}). Laboratory studies have revealed that anthropogenic pollutants, such as sulfur
28 dioxide (SO₂), oxides of nitrogen (NO_x), and aerosol acidity, can enhance SOA formation from
29 the hydroxyl radical (OH)-initiated oxidation of isoprene; however, the mechanisms by which
30 specific pollutants enhance isoprene SOA in ambient PM_{2.5} remain unclear. As one aspect of an
31 investigation to examine how anthropogenic pollutants influence isoprene-derived SOA
32 formation, high-volume PM_{2.5} filter samples were collected at the Birmingham, Alabama (BHM)
33 ground site during the 2013 Southern Oxidant and Aerosol Study (SOAS). Sample extracts were
34 analyzed by gas chromatography/electron ionization-mass spectrometry (GC/EI-MS) with prior
35 trimethylsilylation and ultra performance liquid chromatography coupled to an electrospray
36 ionization high-resolution quadrupole time-of-flight mass spectrometry (UPLC/ESI-HR-
37 QTOFMS) to identify known isoprene SOA tracers. Tracers quantified using both surrogate and
38 authentic standards were compared with collocated gas- and particle-phase data as well as
39 meteorological data provided by the Southeastern Aerosol Research and Characterization
40 (SEARCH) network to assess the impact of anthropogenic pollution on isoprene-derived SOA
41 formation. Results of this study reveal that isoprene-derived SOA tracers contribute a substantial
42 mass fraction of organic matter (OM) (~7 to ~20%). Isoprene-derived SOA tracers correlated with
43 sulfate (SO₄²⁻) ($r^2 = 0.34$, $n = 117$), but not with NO_x. Moderate correlation between methacrylic
44 acid epoxide and hydroxymethyl-methyl- α -lactone (MAE/HMML)-derived SOA tracers and
45 nitrate radical production (P[NO₃]) ($r^2 = 0.57$, $n = 40$) were observed during nighttime, suggesting
46 a potential role of NO₃ radical in forming this SOA type. However, the nighttime correlation of



47 these tracers with nitrogen dioxide (NO_2) ($r^2 = 0.26$, $n = 40$) was weaker. Ozone (O_3) correlated
48 strongly with MAE/HMML-derived tracers ($r^2 = 0.72$, $n = 30$) and moderately with 2-methyltetrols
49 ($r^2 = 0.34$, $n = 15$) during daytime only, suggesting that a fraction of SOA formation could occur
50 from isoprene ozonolysis in urban areas. No correlation was observed between aerosol pH and
51 isoprene-derived SOA. Lack of correlation between aerosol acidity and isoprene-derived SOA
52 indicates that acidity is not a limiting factor for isoprene SOA formation at the BHM site as
53 aerosols were acidic enough to promote multiphase chemistry of isoprene-derived epoxides
54 throughout the duration of the study. All in all, these results confirm the reports that anthropogenic
55 pollutants enhance isoprene-derived SOA formation.



56 1. Introduction

57 Fine particulate matter, suspensions of liquid or solid aerosol in a gaseous medium that are
58 less than or equal to 2.5 μm in diameter ($\text{PM}_{2.5}$), play a key role in physical and chemical
59 atmospheric processes. They influence climate patterns both directly, through the absorption and
60 scattering of solar and terrestrial radiation, and indirectly, through cloud formation (Kanakidou et
61 al., 2005). In addition to climatic effects, $\text{PM}_{2.5}$ has been demonstrated to pose a potential human
62 health risk through inhalation exposure (Pope and Dockery, 2006; Hallquist et al., 2009). Despite
63 the strong association of $\text{PM}_{2.5}$ with climate change and environmental health, there remains a need
64 to more fully resolve its composition, sources, and chemical formation processes in order to
65 develop effective control strategies to address potential hazards in a cost-effective manner
66 (Hallquist et al., 2009; Boucher et al., 2013; Nozière et al., 2015).

67 Atmospheric $\text{PM}_{2.5}$ are comprised in a large part (up to 90% by mass in some locations),
68 of organic matter (OM) (Carlton et al., 2009; Hallquist et al., 2009). OM can be derived from many
69 sources. Primary organic aerosol (POA) is emitted from both natural (e.g., fungal spores,
70 vegetation, vegetative detritus) and anthropogenic sources (fossil fuel and biomass burning) prior
71 to atmospheric processing. As a result of large anthropogenic sources, POA is abundant largely in
72 urban areas. Processes such as biomass burning and combustion also yield volatile organic
73 compounds (VOCs), which have high vapor pressures and can undergo atmospheric oxidation to
74 form secondary organic aerosol (SOA) through gas-to-particle phase partitioning (condensation or
75 nucleation) with subsequent particle-phase (multiphase) chemical reactions (Grieshop et al.,
76 2009).

77 At around 600 Tg emitted per year into the atmosphere, isoprene (2-methyl-1,3-butadiene,
78 C_5H_8) is the most abundant volatile non-methane hydrocarbon (Guenther et al., 2012). The



79 abundance of isoprene is particularly high in the southeastern U.S. due to emissions from broadleaf
80 deciduous tree species (Guenther et al., 2006). Research over the last decade has revealed that
81 isoprene, via hydroxyl radical (OH)-initiated oxidation, is a major source of SOA (Claeys et al.,
82 2004; Edney et al., 2005; Kroll et al., 2005 ; Kroll et al., 2006; Surratt et al., 2006; Lin et al., 2012;
83 Lin et al., 2013a). In addition, it is known that SOA formation is enhanced by anthropogenic
84 emissions, namely oxides of nitrogen (NO_x) and sulfur dioxide (SO₂), that are a source of acidic
85 aerosol onto which photochemical oxidation products of isoprene are reactively taken up to yield
86 a variety of SOA products (Edney et al., 2005; Kroll et al., 2006; Surratt et al., 2006; Surratt et al.,
87 2007b; Surratt et al., 2010; Lin et al., 2013b;).

88 Recent work has begun to elucidate some of the critical intermediates of isoprene oxidation
89 that lead to SOA formation through acid-catalyzed heterogeneous chemistry (Kroll et al., 2005;
90 Surratt et al., 2006). Under low-NO_x conditions, such as in a pristine environment, isomeric
91 isoprene epoxydiols (IEPOX) have been demonstrated to be critical to the formation of isoprene
92 SOA. On advection of IEPOX to an urban environment and mixing with anthropogenic emissions
93 of acidic sulfate aerosol, SOA formation is enhanced (Surratt et al., 2006; Lin et al., 2012; Lin et
94 al., 2013b). This pathway has been shown to yield 2-methyltetrols as major SOA constituents of
95 ambient PM_{2.5} (Claeys et al, 2004; Surratt et al., 2010; Lin et al., 2012). Further work has revealed
96 a number of additional IEPOX-derived SOA tracers, including C₅-alkene triols (Wang et al., 2005;
97 Lin et al., 2012), *cis*- and *trans*-3-methyltetrahydrofuran-3,4-diols (3-MeTHF-3,4-diols) (Lin et
98 al., 2012; Zhang et al., 2012), IEPOX-derived organosulfates (OSs) (Lin et al., 2012), and IEPOX-
99 derived oligomers (Lin et al., 2014). Some of the IEPOX-derived oligomers have been shown to
100 contribute to aerosol components known as brown carbon that absorb light in the near ultraviolet
101 (UV) and visible ranges (Lin et al., 2014). Under high-NO_x conditions, such as encountered in an



102 urban environment, isoprene is oxidized to methacrolein and SOA formation occurs via the further
103 oxidation of methacrolein (MACR) (Kroll et al., 2006; Surratt et al., 2006) to methacryloyl
104 peroxyxynitrate (MPAN) (Chan et al., 2010; Surratt et al., 2010; Nguyen et al., 2015). It has recently
105 been shown that when MPAN is oxidized by OH it yields at least two SOA precursors, methacrylic
106 acid epoxide (MAE) and hydroxymethyl-methyl- α -lactone (HMML) (Surratt et al., 2006; Surratt
107 et al., 2010; Lin et al., 2013a; Nguyen et al., 2015). Whether SOA precursors are formed under
108 high- or low-NO_x conditions, aerosol acidity is a critical parameter that enhances the reaction
109 kinetics through acid-catalyzed reactive uptake and multiphase chemistry of either IEPOX or
110 MAE/HMML (Surratt et al., 2007b; Surratt et al., 2010; Lin et al., 2013b).

111 Due to the considerable emissions of isoprene, an SOA yield of even 1% would contribute
112 significantly to ambient SOA (Carlton et al., 2009; Henze et al., 2009). This conclusion is
113 supported by measurements showing that up to a third of total fine OA mass can be attributed to
114 IEPOX-derived SOA tracers in Atlanta, GA (JST) during summer months (Budisulistiorini et al.,
115 2013; Budisulistiorini et al., 2015). A recent study in Yorkville, GA (YRK), similarly found that
116 IEPOX-derived SOA tracers comprised 12-19% of the fine OA mass (Lin et al., 2013b). Another
117 SOAS site at Centreville, Alabama (CTR) revealed IEPOX-SOA contributed 18% of total OA
118 mass (Xu et al., 2015). The individual ground sites corroborate recent aircraft-based measurements
119 made in the Studies of Emissions and Atmospheric Composition, Clouds, and Climate Coupling
120 by Regional Surveys (SEAC4RS) aircraft campaign, which estimates an IEPOX-SOA contribution
121 of 32% to OA mass in the southeastern U.S. (Hu et al., 2015).

122 It is clear from the field studies discussed above that particle-phase chemistry of isoprene-
123 derived oxidation products plays a large role in atmospheric SOA formation. However, much
124 remains unknown regarding the exact nature of its formation, limiting the ability of models to



125 accurately account for isoprene SOA (Carlton et al., 2010b; Foley et al., 2010). Currently,
126 traditional air quality models in the southeastern U.S. do not incorporate detailed particle-phase
127 chemistry of isoprene oxidation products (IEPOX or MAE/HMML) and generally under-predict
128 isoprene SOA formation (Carlton et al., 2010a). Recent work demonstrates that incorporating the
129 specific chemistry of isoprene epoxide precursors into models increases the accuracy of isoprene
130 SOA prediction (Pye et al., 2013; Karambelas et al., 2014), suggesting that understanding the
131 formation mechanisms of biogenic SOA, especially with regard to the effects of anthropogenic
132 emissions, such as NO_x and SO₂, will be key to more accurate models. More accurate models are
133 needed in order to devise cost-effective control strategies for reducing PM_{2.5} levels. Since isoprene
134 is primarily biogenic in origin, and therefore not controllable, the key to understanding the public
135 health and environmental implications of isoprene SOA lies in resolving the effects of
136 anthropogenic pollutants.

137 This study presents results from the 2013 Southeastern Oxidant and Aerosol Study
138 (SOAS), where several well-instrumented ground sites dispersed throughout the southeastern U.S.
139 made intensive gas- and particle-phase measurements from June 1 – July 16, 2013. The primary
140 purpose of this campaign was to examine, in greater detail, the formation mechanisms,
141 composition, and properties of biogenic SOA, including the effects of anthropogenic emissions.
142 This study pertains specifically to the results from the BHM ground site, where the city's ample
143 urban emissions mix with biogenic emissions from the surrounding rural areas, creating an ideal
144 location to investigate such interactions. The results presented here focus on analysis of PM_{2.5}
145 collected on filters during the campaign by gas chromatography interfaced to electron ionization-
146 mass spectrometry (GC/EI-MS) and ultra performance liquid chromatography interfaced with
147 electrospray ionization high-resolution quadrupole time-of-flight mass spectrometry (UPLC/ESI-



148 HR-QTOFMS). The analysis of $PM_{2.5}$ was conducted in order to measure quantities of known
149 isoprene SOA tracers and using collocated air quality and meteorological measurements to
150 investigate how anthropogenic pollutants including NO_x , SO_2 , aerosol acidity (pH), $PM_{2.5}$ sulfate
151 (SO_4^{2-}), and O_3 affect isoprene SOA formation. These results, along with the results presented
152 from similar studies during the 2013 SOAS campaign, seek to elucidate the chemical relationships
153 between anthropogenic emissions and isoprene SOA formation in order to provide better
154 parameterizations needed to improve the accuracy of air quality models in this region of the U.S.

155 **2. Methods**

156 **2.1. Site description and collocated data**

157 Filter samples were collected in the summer of 2013 as part of the SOAS field campaign
158 at the BHM ground site (33.553N, 86.815W). In addition to the SOAS campaign, the site is also
159 part of the Southeastern Aerosol Research and Characterization Study (SEARCH) (Figure S1 of
160 the Supplement), an observation and monitoring program initiated in 1998. SEARCH and this site
161 are described elsewhere in detail (Hansen et al., 2003; Edgerton et al., 2006). The BHM site is
162 surrounded by significant transportation and industrial sources of PM. West of BHM are US-31
163 and I-65 highways. To the north, northeast and southwest of BHM several coking ovens and an
164 iron pipe foundry are located (Hansen et al., 2003).

165 **2.2. High-Volume filter sampling and analysis methods**

166 **2.2.1. High-Volume filter sampling**

167 From June 1 – July 16, 2013, $PM_{2.5}$ samples were collected onto Tissuquartz™ Filters
168 (8 x 10 in, Pall Life Sciences) using high-volume $PM_{2.5}$ samplers (Tisch Environmental) operated
169 at $1\text{ m}^3\text{ min}^{-1}$ at ambient temperature described in detail elsewhere (Budisulistiorini et al. 2015;



170 Riva et al., 2015). All quartz filters were pre-baked prior to collection. The procedure consisted of
171 baking filters at 550 °C for 18 hours followed by cooling to 25 °C over 12 hours.

172 The sampling schedule is given in Table 1. Either two or four samples were collected per
173 day. The regular schedule consisted of two samples per day, one during the day, the second at
174 night, each collected for 11 hours. On intensive sampling days, four samples were collected, with
175 the single daytime sample being subdivided into three separate periods. The intensive sampling
176 schedule was conducted on days when high levels of isoprene, SO_4^{2-} and NO_x were forecast by
177 the National Center for Atmospheric Research (NCAR) using the Flexible Particle dispersion
178 model (FLEXPART) (Stohl et al., 2005) and Model for Ozone and Related Chemical Tracers
179 (MOZART) (Emmons et al., 2010) simulations. Details of these simulations have been
180 summarized in Budisulistiorini et al. (2015); however, these model data were only used
181 qualitatively to determine the sampling schedule. The intensive collection frequency allowed
182 enhanced time resolution for offline analysis to examine the effect of anthropogenic emissions on
183 the evolution of isoprene SOA tracers throughout the day.

184 In total, 120 samples were collected throughout the field campaign with a field blank filter
185 collected every 10 days to identify errors or contamination in sample collection and analysis. All
186 filters were stored at -20 °C in the dark until extraction and analysis. In addition to filter sampling
187 of $\text{PM}_{2.5}$, SEARCH provided a suite of additional instruments at the site collecting measurements
188 of a variety of variables, including meteorology, gas, and continuous PM monitoring. The variables
189 with respective instrumentation are summarized in Table S1 of the Supplement.

190 2.2.2. Isoprene-derived SOA analysis by GC/EL-MS



191 SOA collected in the field on quartz filters was extracted and isoprene tracers quantified
192 by GC/EI-MS with prior trimethylsilylation. A 37-mm diameter circular punch from each filter
193 was extracted in a pre-cleaned scintillation vial with 20 mL of high-purity methanol (LCMS
194 CHROMASOLV-grade, Sigma-Aldrich) by sonication for 45 minutes. The extracts were filtered
195 through PTFE syringe filters (Pall Life Science, Acrodisc®, 0.2- μ m pore size) to remove insoluble
196 particles and residual quartz fibers. The filtrate was then blown dry under a gentle stream of N₂ at
197 room temperature. The dried residues were immediately trimethylsilylated by reaction with 100
198 μ L of BSTFA + TMCS (99:1 v/v, Supelco) and 50 μ L of pyridine (anhydrous, 99.8 %, Sigma-
199 Aldrich) at 70 °C for 1 hour. Derivatized samples were analyzed within 24 hours after
200 trimethylsilylation using a Hewlett-Packard (HP) 5890 Series II Gas Chromatograph coupled to a
201 HP 5971A Mass Selective Detector. The gas chromatograph was equipped with an *Econo-Cap*®-
202 *EC*®-5 Capillary Column (30 m x 0.25 mm i.d.; 0.25- μ m film thickness) to separate trimethylsilyl
203 derivatives before MS detection. 1 μ L aliquots were injected onto the column. Operating
204 conditions and procedures have been described elsewhere (Surratt et al., 2010).

205 Extraction efficiency was assessed and taken into account for the quantification of all SOA
206 tracers. Efficiency was determined by analyzing 4 pre-baked filters spiked with 50 ppmv of 2-
207 methyltetrols, 2-methylglyceric acid, levoglucosan, and *cis*- and *trans*-3-MeTHF-3,4-diols.
208 Extraction efficiency was above 90% and used to correct the quantification of samples. Extracted
209 ion chromatograms (EICs) of *m/z* 262, 219, 231, 335 were used to quantify the *cis*-/*trans*-3-
210 MeTHF-3,4-diols, 2-methyltetrols and 2-methylglyceric acid, C₅-alkene triols, and IEPOX-
211 dimers, respectively (Surratt et al., 2006).

212 2-Methyltetrols were quantified using an authentic reference standard that consisted of a
213 mixture of racemic diastereoisomers. Similarly, 3-MeTHF-3,4-diol isomers were also quantified



214 using authentic standards; however, 3-MeTHF-3,4-diol isomers were detected in few field
215 samples. 2-Methylglyceric acid was also quantified using an authentic standard. Procedures for
216 synthesis of the 2-methyltetrols, 3-MeTHF-3,4-diol isomers, and 2-methylglyceric acid have been
217 described elsewhere (Zhang et al., 2012; Budisulistiorini et al., 2015). C₅-alkene triols and IEPOX-
218 dimers were quantified using the average response factor of the 2-methyltetrols.

219 **2.2.3. Isoprene-derived SOA analysis by UPLC/ ESI-HR-QTOFMS**

220 A 37-mm diameter circular punch from each quartz filter was extracted following the same
221 procedure described in section 2.2.1 for GC/EI-MS analysis. The dried residues were reconstituted
222 with 150 μ l of a 50:50 (v/v) solvent mixture of methanol (LC-MS CHROMASOVL-grade, Sigma-
223 Aldrich) and high-purity water (Milli-Q, 18.2 M Ω). The extracts were immediately analyzed by
224 the UPLC/ESI-HR-QTOFMS (6520 Series, Agilent) operated in the negative ion mode. Detailed
225 operating conditions have been described elsewhere (Riva et al., 2015). Mass spectra were
226 acquired at a mass resolution 7000-8000 over the range m/z 200 – 400.

227 Extraction efficiency was determined by analyzing 3 pre-baked filters spiked with propyl
228 sulfate and octyl sulfate (electronic grade, City Chemical LLC). Extraction efficiencies were in the
229 range 86 – 95%. EICs of m/z 215, 333 and 199 were used to quantify the IEPOX-derived OS,
230 IEPOX-derived dimer OS and the MAE/HMML-derived OS, respectively (Surratt et al., 2007a).
231 EICs were generated with a \pm 5 ppm tolerance. All accurate masses for all measured
232 organosulfates were within \pm 5 ppm. For simplicity, only the nominal masses are reported in the
233 text when describing these products. IEPOX-derived OS and IEPOX-derived dimer OS were
234 quantified by authentic standards (Zhang et al., 2012). The MAE/HMML-derived OS was
235 quantified using authentic MAE/HMML-derived OS synthesized in-house by a procedure to be
236 described in a forthcoming publication (¹H NMR trace, Figure S2).



237 EICs of m/z 155, 169 and 139 were used to quantify the glyoxal-derived OS,
238 methylglyoxal-derived OS, and the hydroxyacetone-derived OS, respectively (Surratt et al.,
239 2007a). In addition, EICs of m/z 211, 260 and 305 were used to quantify other known isoprene-
240 derived OSs (Surratt et al., 2007a). Glycolic acid sulfate synthesized in-house was used as a
241 standard to quantify the glyoxal-derived OS (Galloway et al., 2009) and propyl sulfate, was used
242 as a surrogate standard to quantify the remaining isoprene-derived OSs.

243 **2.2.4. OC and WSOC analysis**

244 A 1.5 cm² square punch from each quartz filter was analyzed for total organic carbon (OC)
245 and elemental carbon (EC) by the thermal-optical method (Birch and Cary, 1996) on a Sunset
246 Laboratory OC/EC instrument (Tigard, OR) at the National Exposure Research Laboratory
247 (NERL) at the U.S. Environmental Protection Agency, Research Triangle Park, NC. The details
248 of the instrument and analytical method have been described elsewhere (Birch and Cary, 1996). In
249 addition to the internal calibration using methane gas, four different mass concentrations of sucrose
250 solution were used to verify the accuracy of instrument during the analysis.

251 Water-soluble organic carbon (WSOC) was measured in aqueous extracts of quartz fiber filter
252 samples using a total organic carbon (TOC) analyzer (Sievers 5310C, GE Water & Power)
253 equipped with an inorganic carbon remover (Sievers 900). To maintain low background carbon
254 levels, all glassware used was washed with water, soaked in 10% nitric acid, and baked at 500°C
255 for 5 h and 30 min prior to use. Samples were extracted in batches that consisted of 12-21 PM_{2.5}
256 samples and field blanks, one laboratory blank, and one spiked solution. A 17.3 cm² filter portion
257 was extracted with 15 mL of purified water (> 18 MΩ, Barnstead Easypure II, Thermo Scientific)
258 by ultra-sonication (Branson 5510). Extracts were then passed through a 0.45 μm PTFE filter to
259 remove insoluble particles. The TOC analyzer was calibrated using potassium hydrogen phthalate



260 (KHP, Sigma Aldrich) and was verified daily with sucrose (Sigma Aldrich). Samples and standards
261 were analyzed in triplicate; the reported values correspond to the average of the second and third
262 trials. Spiked solutions yielded recoveries that averaged (\pm one standard deviation) 96 ± 5 % ($n =$
263 9). All ambient concentrations were field blank subtracted.

264 **2.2.5. Estimation of aerosol pH by ISORROPIA**

265 Aerosol pH was estimated using a thermodynamic model, ISORROPIA-II (Nenes et al.,
266 1998). SO_4^{2-} , nitrate (NO_3^-), and ammonium (NH_4^+) ion concentrations measured in $\text{PM}_{2.5}$
267 collected from BHM, as well as relative humidity (RH), temperature and gas-phase ammonia
268 (NH_3) were used as inputs into the model. These variables were obtained from the SEARCH
269 network at BHM, which collected the data during the period covered by the SOAS campaign. The
270 ISORROPIA-II model estimates particle hydronium ion concentration per unit volume of air (H^+ ,
271 $\mu\text{g m}^{-3}$), aerosol liquid water content (LWC, $\mu\text{g m}^{-3}$), and aqueous aerosol mass concentration (μg
272 m^{-3}). The model-estimated parameters were used in the following formula to calculate the aerosol
273 pH:

$$274 \quad \text{Aerosol pH} = -\log_{10} a_{\text{H}^+} = -\log_{10} \left(\frac{H_{\text{air}}^+}{LMASS} \times \rho_{\text{aer}} \times 1000 \right)$$

275 where a_{H^+} is H^+ activity in the aqueous phase (mol L^{-1}), $LMASS$ is total liquid-phase aerosol mass
276 ($\mu\text{g m}^{-3}$) and ρ_{aer} is aerosol density. Details of the ISORROPIA-II model and its ability to predict
277 pH, LWC, and gas-to-particle partitioning are not the focus of this study and are discussed
278 elsewhere and (Fountoukis et al., 2009).

279 **2.2.6. Estimation of nighttime NO_3**

280 Nitrate radical (NO_3) production ($\text{P}[\text{NO}_3]$) was calculated using the following equation:



281
$$P[NO_3] = [NO_2][O_3]k$$

282 where $[NO_2]$ and $[O_3]$ correspond to the measured ambient NO_2 and O_3 concentrations (mol
283 cm^{-3}), respectively, and k is the temperature-dependent rate constant (Herron and Huie, 1974;
284 Graham and Johnston, 1978). Since no direct measure of NO_3 radical was made at this site during
285 SOAS, $P[NO_3]$ was used as a proxy for NO_3 radicals present in the atmosphere to examine if there
286 is any association of it with isoprene-derived SOA tracers.

287 3. Results and Discussion

288 3.1. Overview of the study

289 The campaign extended from June 1 through July 16, 2013. Temperature during this period
290 ranged from a high of 32.6 °C to a low of 20.5 °C, with an average of ~26.4 °C. RH varied from
291 37-96% throughout the campaign, with an average of 71.5%. Rainfall occurred intermittently over
292 2-3 day periods and averaged 0.1 inches per day. Wind analysis reveals that air masses approached
293 largely from the south-southeast at an average wind speed of 2 $m s^{-1}$. Summaries of meteorological
294 conditions as well as wind speed and direction during the course of the campaign are given in
295 Table 2 and illustrated in Figures 1 and 2.

296 The average concentration of carbon monoxide (CO), a combustion byproduct, was 208.7
297 ppbv. The mean concentration of O_3 was significantly higher (*t-test*, *p-value* < 0.05) on intensive
298 sampling days (37.0 ppbv) than regular sampling days (25.2 ppbv). Concentrations of NO_x , NH_3 ,
299 and SO_2 were lower averaging 7.8, 1.9, and 0.9 ppbv, respectively. On average, OC and WSOC
300 levels were 7.2 ($n = 120$) and 4 $\mu g m^{-3}$ ($n = 100$), respectively. The largest inorganic component of
301 $PM_{2.5}$ was SO_4^{2-} , which averaged 2 $\mu g m^{-3}$ with excursions between 0.4 and 4.9 $\mu g m^{-3}$ during the
302 campaign. NH_4^+ and NO_3^- were present at low levels, averaging 0.66 and 0.14 $\mu g m^{-3}$, respectively.
303 Time series of gas and $PM_{2.5}$ components are shown in Figure 2. WSOC accounted for 35% of OC



304 mass (Figure S3a), and was smaller than that recently reported in rural areas during SOAS
305 (Budisulistiorini et al., 2015; Hu et al., 2015), but consistent with previous observations at the
306 BHM site (Ding et al., 2008). WSOC/OC ratios are commonly lower in urban than rural areas, as
307 a consequence of higher primary OC emissions; thus, PM at BHM probably contains increased
308 OC.

309 Diurnal variation of meteorological parameters, trace gases, and PM_{2.5} components are
310 shown in Figure S4 of the Supplement. Temperature dropped during nighttime, and reached a
311 maximum in the afternoon (Figure S4a). Conversely, RH was low during day and high at night.
312 High-NO_x levels were found in the early morning and decreased during the course of the day
313 (Figure S4c), most likely in conjunction with rising O₃ levels. O₃ reached a maximum
314 concentration between 12 - 3 pm due to photochemistry (Figure S4b). SO₂ was slightly higher in
315 the morning (Figure S4c), but decreased during the day most likely as a result of planetary
316 boundary layer (PBL) dynamics. NH₃ remained fairly constant throughout the day (Figure S4c).
317 No significant diurnal variation was found in the concentration of inorganic PM_{2.5} components,
318 including SO₄²⁻, NO₃⁻, and NH₄⁺ (Figure S4d). Unfortunately, a measurement of isoprene could
319 not be made at BHM during the campaign. However, the diurnal trend of isoprene levels might be
320 similar to the data at the CTR site (Xu et al., 2015), which is only 61 miles away from BHM. Xu
321 et al. (2015) observed the highest levels of isoprene (~ 6 ppb) at CTR in the mid-afternoon (3 pm
322 local time) and its diurnal trend was similar to isoprene-OA measured by the Aerodyne Aerosol
323 Mass Spectrometer (AMS) during the SOAS campaign.

324 **3.2 Characterization of Isoprene SOA**

325 Table 3 summarizes the mean and maximum concentrations of known isoprene-derived
326 SOA tracers detected by GC/EI-MS and UPLC/ESI-HR-QTOFMS. Levoglucosan was also



327 analyzed as a tracer for biomass burning. Among the isoprene-derived SOA tracers, the highest
328 mean concentration was for 2-methyltetrols (376 ng m^{-3}), followed by the sum of C₅-alkene triols
329 (181 ng m^{-3}) and the IEPOX-derived OS (165 ng m^{-3}). The concentrations account for 3.8%, 1.8%
330 and 1.6%, respectively, of total OM mass. Noteworthy is that maximum concentrations of 2-
331 methylerythritol (a 2-methyltetrol isomer; 1049 ng m^{-3}), IEPOX-derived OS (865 ng m^{-3}) and (E)-
332 2-methylbut-3-ene-1,2,4-triol (879 ng m^{-3}) were attained during the intensive sampling period 4-7
333 pm local time on June 15, 2013, following five consecutive days of dry weather (Figure 2a and
334 2d) when high levels of isoprene, SO_4^{2-} , and NO_x were forecast.

335 Together, the IEPOX-derived SOA tracers, which represent SOA formation from isoprene
336 oxidation predominantly under the low- NO_x pathway, comprised 92.5% of the total detected
337 isoprene-derived SOA tracer mass at the BHM site. This contribution is slightly lower than
338 observations reported at rural sites located in Yorkville, GA (97.5%) and Look Rock, Tennessee
339 (LRK) (97%) (Lin et al., 2013b; Budisulistiorini et al., 2015).

340 The sum of MAE/HMML-OS and 2-MG, which represent SOA formation from isoprene
341 oxidation predominantly under the high- NO_x pathway, contributed 3.25% of the total isoprene-
342 derived SOA tracer mass, while the OS derivative of glycolic acid (GA sulfate) contributed 3.3%.
343 The contribution of GA sulfate was consistent with the level of GA sulfate measured by the
344 airborne NOAA Particle Analysis Laser Mass Spectrometer (PALMS) over the continental U.S.
345 during the Deep Convective Clouds and Chemistry Experiment and SEAC4RS (Liao et al., 2015).
346 However, the contribution of GA sulfate to the total OM at BHM (0.3%) is lower than aircraft-
347 based measurements made by Liao et al. (2015) near the ground in the eastern U.S. (0.9%). GA
348 sulfate can form from biogenic and anthropogenic emissions other than isoprene, including



349 glyoxal, which is thought to be a primary source of GA sulfate (Galloway et al., 2009). For this
350 reason, GA sulfate will not be further discussed in this study.

351 Isoprene SOA contribution to total OM was estimated by assuming the OM/OC ratio 1.6
352 based on the recent studies (El-Zanan et al., 2009; Simon et al., 2011; Ruthenburg et al., 2014;
353 Blanchard et al., 2015). On average, isoprene-derived SOA tracers (sum of both IEPOX- and
354 MAE/HMML-derived SOA tracers) contributed ~7% (ranging to ~ 20% at times) of the total
355 particulate OM mass. The average contribution is lower than measured at other sites in the S.E.
356 USA, including both rural LRK, (Budisulistiorini et al., 2015; Hu et al., 2015) and urban Atlanta,
357 GA (Budisulistiorini et al., 2013). The contribution of SOA tracers to OM in the current study was
358 estimated on the basis of offline analysis of filters, while tracer estimates in the two earlier studies
359 was based on online ACSM/AMS measurements. The low isoprene SOA/OM ratio is consistent
360 with the low WSOC/OC reported in section 3.1, suggesting an increased contribution of primary
361 OA or secondary OM to the total OM at BHM. However, it should be noted that total IEPOX-
362 derived SOA mass at BHM may actually be closer to ~14% since recent measurements by the
363 Aerodyne ACSM at LRK indicated that tracers could only account for ~50% of the total IEPOX-
364 derived SOA mass resolved by the ACSM (Budisulistiorini et al., 2015). Unfortunately, an
365 Aerodyne ACSM or AMS was not available at the BHM site, precluding confirmation of that
366 IEPOX-derived SOA mass at BHM might account for 14% (on average) of the total OM mass.
367 Levoglucosan, a biomass-burning tracer, averaged 1% of total OM with spikes up to 8%, the same
368 level measured for 2-methylthreitol and (E)-2-methylbut-3-ene-1,2,4-triol (Table 3). The ratio of
369 average levoglucosan at BHM relative to CTR was 5.4 suggesting significantly more biomass
370 burning impacting the BHM site.



371 IEPOX- and MAE/HMML-derived SOA tracers accounted for 18% and 0.4% of the
372 WSOC mass, respectively (Figure S3b), lower than the respective contributions of 24% and 0.7%
373 measured at LRK (Budisulistiorini et al., 2015).

374 Figure S5 shows no diurnal variation for the average day and night concentrations of
375 isoprene-derived SOA tracers. Thus cooler nighttime temperatures also do not appear to enhance
376 gas-to-particle partitioning at the BHM site. Figures S6 and S7 show the variation of isoprene-
377 derived SOA tracers during intensive sampling periods. The highest concentrations were usually
378 observed in samples collected from 4 pm – 7 pm, local time; however, no statistical significance
379 were observed between intensive periods. This observation illustrates the importance of the higher
380 time-resolution of the tracer data during intensive sampling periods over course of the campaign
381 (Table S2-S6). An additional consequence of the intensive sampling periods was resolution of a
382 significant correlation between isoprene SOA tracers and O₃ to be discussed in more detail in
383 section 3.3.2.

384 **3.3 Influence of anthropogenic emissions on isoprene-derived SOA**

385 **3.3.1 Effects of reactive nitrogen-containing species**

386 During the campaign, no isoprene-derived SOA tracers, including MAE/HMML-derived
387 OS and 2-MG, correlated with NO_x or NO_y ($r^2 = 0$, $n = 120$). This is inconsistent with the current
388 understanding of SOA formation from isoprene oxidation pathways under high-NO_x conditions,
389 which proceeds through uptake of MAE (Lin et al., 2013a), and, as recently suggested, HMML
390 (Nguyen et al., 2015), to yield 2-MG and its OS derivative. Plume age, as a ratio of NO_x:NO_y, in
391 this study was highly correlated with O₃ ($r^2 = 0.79$, $n = 120$). This correlation might be explained
392 by the photolysis of NO₂, which is abundant due to traffic at the urban ground site, resulting in



393 formation of tropospheric O₃. A negative correlation coefficient ($r = -0.47$, $n = 120$) between
394 plume age and 2-MG abundance was found, suggesting that formation of some 2-MG may be
395 associated with ageing of air masses.

396 A previous study supported a major role for NO₃ in the nighttime chemistry of isoprene
397 (Ng et al., 2008). Correlation of IEPOX- and MAE/HMML-derived SOA with nighttime NO₂, O₃,
398 and P[NO₃] were examined in this study (Figures 3 and 4). As shown in Figure 3f, a moderate
399 correlation between MAE/HMML-derived SOA and nighttime P[NO₃] ($r^2 = 0.57$, $n = 40$) was
400 observed. The regression analysis revealed a significant correlation at the 95% confidence interval
401 (p -value < 0.05) (Table S7). This finding suggests that some MAE/HMML-derived SOA may form
402 locally from the reaction of isoprene with NO₃ radical at night. A field study reported a peak
403 isoprene mixing ratio in early evening (Starn et al., 1998) as the PBL height decreases at night. As
404 a result, lowering PBL heights could concentrate the remaining isoprene, NO₂, and O₃ that can
405 continue to react during the course of the evening. 2-MG formation has been reported to be NO₂-
406 dependent via the formation and further oxidation of MPAN (Surratt et al., 2006; Chan et al.,
407 2010). Hence, decreasing PBL may be related to nighttime MAE/HMML-derived SOA formation
408 through isoprene oxidation by both P[NO₃] and NO₂.

409 Although P[NO₃] depends on both NO₂ and O₃ levels, O₃ correlates moderately with
410 MAE/HMML-derived SOA tracers during day ($r^2 = 0.48$, $n = 75$), but not at night ($r^2 = 0.08$, $n =$
411 45). The effect of O₃ on isoprene-derived SOA formation during daytime will be discussed further
412 in section 3.3.2. NO₂ levels correlate only weakly with MAE/HMML-derived SOA tracers, ($r^2 =$
413 0.26, $n = 45$) indicating that NO₂ levels alone do not explain the moderate correlation of P[NO₃]
414 with these tracers. To our knowledge, correlation of P[NO₃] with high-NO_x SOA tracers has not



415 been observed in previous field studies., indicating that further work is needed to examine the
416 potential role of nighttime NO_3 radicals in forming these SOA tracers.

417 As shown in Figure 4f, IEPOX-derived SOA was weakly correlated ($r^2 = 0.26$, $n = 40$) with
418 nighttime $\text{P}[\text{NO}_3]$. The correlation appears to be driven by the data at the low end of the scale and
419 could therefore be misleading. However, Schwantes et al. (2015) demonstrated that NO_3 -initiated
420 oxidation of isoprene yields isoprene nitrooxy hydroperoxides (INEs) through nighttime reaction:
421 $\text{RO}_2 + \text{HO}_2$, which on further oxidation yielded isoprene nitrooxy hydroxyepoxides (INHEs). The
422 INHEs undergo reactive uptake onto acidic sulfate aerosol to yield SOA constituents similar to
423 those of IEPOX-derived SOA. The present study raises the possibility that a fraction of IEPOX-
424 derived SOA comes from NO_3 -initiated oxidation of isoprene at night. The work of Ng et al.
425 (2008) does not explain the weak association we observe here between IEPOX-derived SOA
426 tracers and $\text{P}[\text{NO}_3]$ as a consequence of the reactions $\text{RO}_2 + \text{RO}_2$ and $\text{RO}_2 + \text{NO}_3$ reactions
427 dominating in those experiments. It is now thought that $\text{RO}_2 + \text{HO}_2$ should dominate in field studies
428 (Schwantes et al., 2015; Paulot et al., 2009).

429 3.3.2 Effect of O_3

430 During the daytime, O_3 was moderately correlated ($r^2 = 0.48$, $n = 75$) with total
431 MAE/HMML-derived SOA (Figure 3b). This correlation was stronger ($r^2 = 0.72$, $n = 30$, *p-value*
432 < 0.05 , Table S7) when filters taken during regular daytime sampling periods are considered,
433 suggesting that formation of MACR (a precursor to MAE and HMML) (Lin et al., 2013b; Nguyen
434 et al., 2015) was enhanced by oxidation of isoprene by O_3 (Kamens et al., 1982). O_3 was not
435 correlated ($r^2 = 0.08$, $n = 45$) with MAE/HMML-derived SOA at night (Figure 3e). The latter
436 finding is consistent with the absence of photolysis to drive the production of O_3 . However,



437 residual O₃ may play an important role at night to form MAE/HMML-derived SOA via the P[NO₃]
438 pathway discussed in section 3.3.1.

439 O₃ was not correlated ($r^2 = 0.10$, $n = 75$) with IEPOX-derived SOA during daytime (Figure
440 4b), but weakly correlated with 2-methylerythritol ($r^2 = 0.25$, $n = 30$) as shown in Table S2,
441 especially during intensive 3 sampling periods ($r^2 = 0.34$, $n = 15$, Table S5). An important
442 observation with regard to this result is that no correlation has been found between O₃ and 2-
443 methyltetrols ($r^2 < 0.01$) in previous field studies (Lin et al., 2013b; Budisulistiorini et al., 2015).
444 Isoprene ozonolysis yielded 2-methyltetrols in chamber studies in the presence of acidified sulfate
445 aerosol (Riva et al., 2015) but C₅-alkene-triols were not formed by this pathway. The greatest
446 abundance of isoprene-derived SOA tracers in daytime samples was generally observed in
447 intensive 3 samples; however, there was no statistical significance observed between intensive
448 samples. The moderate correlation ($r^2 = 0.34$, $n = 15$, p -value < 0.05) between O₃ and the 2-
449 methyltetrols observed in intensive 3 samples occurred when O₃ reached maximum levels,
450 suggesting that ozonolysis of isoprene plays a role in 2-methyltetrol formation. Lack of correlation
451 between O₃ and C₅-alkene triols during intensive 3 sampling ($r^2 = 0.10$, $n = 15$) supports this
452 contention. A putative pathway is formation of hydroperoxides that partition to wet acidic sulfate
453 aerosols and react further to yield 2-methyltetrols. Additional work using authentic standards is
454 needed to validate this tentative hypothesis.

455 3.3.3 Effect of particle SO₄²⁻

456 SO₄²⁻ was moderately correlated with IEPOX-derived SOA ($r^2 = 0.36$, $n = 117$) and
457 MAE/HMML-derived SOA ($r^2 = 0.33$, $n = 117$) at the 95% confidence interval as shown in Table
458 S7. The strength of the correlations was consistent with studies at other sites across the
459 Southeastern U.S. (Budisulistiorini et al., 2013; Lin et al., 2013b; Budisulistiorini et al., 2015; Xu



460 et al., 2015). Aerosol surface area provided by acidic SO_4^{2-} has been demonstrated to control the
461 uptake of isoprene-derived epoxides (Lin et al., 2012; Gaston et al., 2014; Nguyen et al., 2014;
462 Riedel et al., 2015).

463 Furthermore, SO_4^{2-} is proposed to enhance IEPOX-derived SOA formation by providing
464 particle water ($\text{H}_2\text{O}_{\text{ptcl}}$) required for IEPOX uptake (Xu et al., 2015). Aerosol SO_4^{2-} also promotes
465 acid-catalyzed ring-opening reactions of IEPOX by H^+ , proton donors such as NH_4^+ , and
466 nucleophiles (e.g., H_2O , SO_4^{2-} , or NO_3^-) (Surratt et al., 2010; Nguyen et al., 2014). Since SO_4^{2-}
467 tends to drive both particle water and acidity (Fountoukis and Nenes, 2007), the extent to which
468 each influences isoprene SOA formation during field studies remains unclear. Multivariate linear
469 regression analysis on SOAS data from the CTR site and the SCAPE dataset revealed a statistically
470 significant positive linear relationship between SO_4^{2-} and the isoprene (IEPOX)-OA factor
471 resolved by positive matrix factorization (PMF). On the basis of this analysis the abundance of
472 SO_4^{2-} was concluded to control directly the isoprene SOA formation over broad areas of the
473 Southeastern U.S. (Xu et al., 2015), consistent with previous reports (Lin et al., 2013;
474 Budisulistiorini et al., 2013; Budisulistiorini et al., 2015). Another potential pathway for SO_4^{2-}
475 levels to enhance isoprene SOA formation is through salting-in effects; however, systematic
476 investigations of this effect are lacking and further studies are warranted (Xu et al., 2015).

477 **3.3.4 Effect of aerosol acidity**

478 The aerosol at BHM was acidic throughout the SOAS campaign (pH range 1.60 – 1.94,
479 average 1.76) in accord with a study by Guo et. al. (2014) that found aerosol pH ranging from
480 0 – 2 throughout the southeastern U.S. However, no correlation of pH with isoprene SOA
481 formation was observed at BHM, also consistent with previous findings using the thermodynamic



482 models to estimate aerosol acidity in many field sites across the southeastern U.S. region, including
483 Yorkville, GA (YRK) (Lin et al., 2013b), Jefferson Street, GA (JST) (Budisulistiorini et al., 2013),
484 and LRK (Budisulistiorini et al., 2015). However, it is important to point out that the lack of
485 correlation between SOA tracers and acidity may stem from the small variations in aerosol acidity
486 throughout the campaign. Gaston et al. (2014) and Riedel et al. (2015) recently demonstrated that
487 an aerosol $\text{pH} < 2$ at atmospherically-relevant aerosol surface areas would allow reactive uptake
488 of IEPOX onto acidic (wet) sulfate aerosol surfaces to be competitive with other loss processes
489 (e.g., deposition and reaction of IEPOX with OH). In fact, it was estimated that under such
490 conditions IEPOX would have a lifetime of ~ 5 hr. The constant presence of acidic aerosol has
491 also been observed at other field sites in the southeastern U.S. (Budisulistiorini et al., 2013;
492 Budisulistiorini et al., 2015; Xu et al., 2015), supporting a conclusion that acidity is not the limiting
493 variable in forming isoprene SOA.

494 **3.4 Comparison among different sampling sites during 2013 SOAS campaign**

495 Table 5 summarizes the mean concentration and contribution of each isoprene SOA tracer
496 at BHM, CTR, and LRK. BHM is an industrial-residential area, LRK and CTR are rural areas,
497 although LRK is influenced by a diurnal upslope/downslope cycle of air from an urban locality
498 (Knoxville) (Tanner et al., 2005). IEPOX-derived SOA was predominant at all three sites during
499 the SOAS campaign, while MAE/HMML-derived SOA constituted a minor contribution. The
500 average ratio of 2-methyltetrols to C_5 -alkene triols at BHM was 2.2, nearly double that of CTR
501 (1.3) and LRK (1.1). Although 2-methyltetrols and C_5 -alkene triols are considered to form readily
502 from the acid-catalyzed reactive uptake and multiphase chemistry of IEPOX (Edney et al., 2005;
503 Surratt et al., 2006), Riva et al. (2015) recently demonstrated that only 2-methyltetrols can be
504 formed via isoprene ozonolysis in the presence of acidic sulfate aerosol. The higher levels of the



505 2-methyltetrols observed at the urban BHM site indicates a likely competition between the IEPOX
506 uptake and ozonolysis pathways. Together, these findings suggest that urban O₃ may play an
507 important role in forming the 2-methyltetrols observed at BHM. There were notable trends found
508 among the three sites: (1) average C₅-alkene triol concentrations were higher at CTR (214.1 ng m⁻³)
509 ³) than at BHM (169.7 ng m⁻³) and LRK (144.4 ng m⁻³); (2) average isomeric 3-MeTHF-diol
510 concentrations were lower at CTR (0.2 ng m⁻³) than the BHM (15.4 ng m⁻³) or LRK (4.4 ng m⁻³)
511 sites. Except for the 2-methyltetrols, reasons for the differences observed for the other tracers
512 between sites remains unclear and warrant future investigations.

513

514 4. Conclusions

515 This study examined isoprene SOA tracers in PM_{2.5} samples collected at the BHM ground
516 site during the 2013 SOAS campaign and revealed the complexity and potential multitude of
517 chemical pathways leading to isoprene SOA formation. Isoprene SOA contributed up to ~20%
518 (~7% on average) of total OM mass. IEPOX-derived SOA tracers were responsible for 92% of the
519 total quantified isoprene SOA tracer mass, with 2-methyltetrols being the major component (47%).
520 Differences in the relative contributions of IEPOX- and MAE/HMML-derived SOA tracers at
521 BHM and the rural CTR and LRK sites (Budisulistiorini et al., 2015) during the 2013 SOAS
522 campaign, support suggestions that anthropogenic emissions effect isoprene SOA formation. The
523 correlation between 2-methyltetrols and O₃ at BHM is in accord with work by Riva et al. (2015),
524 demonstrating a potential role of O₃ in generating isoprene-derived SOA in addition to the
525 currently accepted IEPOX multiphase pathway.

526 At BHM, the statistical correlation of particulate SO₄²⁻ with IEPOX- ($r^2 = 0.36$, $n = 117$, p
527 < 0.05) and MAE-derived SOA tracers ($r^2 = 0.33$, $n = 117$, $p < 0.05$) suggests that SO₄²⁻ plays a



528 role in isoprene SOA formation. Although none of isoprene-derived SOA tracers correlated with
529 gas-phase NO_x and NO_y , MAE/HMML-derived SOA tracers correlated with nighttime $\text{P}[\text{NO}_3]$ (r^2
530 = 0.57, $n = 400$), indicating that NO_3 may affect local MAE/HMML-derived SOA formation.
531 Nighttime $\text{P}[\text{NO}_3]$ was weakly correlated ($r^2 = 0.26$, $n = 40$) with IEPOX-derived SOA tracers,
532 lending some support to recent work by Schwantes et al. (2015) showing that isoprene + NO_3
533 yields INHEs that can by undergo reactive uptake to yield IEPOX tracers and contribute to IEPOX-
534 derived SOA tracer loadings. In addition, nighttime 2-methyltetrol levels in the urban atmosphere
535 deviate from the conventional understanding of isoprene SOA formation in terms of segregated
536 NO_x dependent regimes. The correlation of daytime O_3 with MAE/HMML-derived SOA and with
537 2-methyltetrols offers a new insight into influences on isoprene SOA formation. Notably, O_3 has
538 not been reported to correlate with isoprene-derived SOA tracers in previous field studies (Lin et
539 al., 2013b; Budisulistiorini et al., 2015). In this study, the strong correlation ($r^2 = 0.72$, $n = 30$) at
540 the 95% confidence interval of O_3 with MAE/HMML-derived SOA tracers during the regular
541 daytime sampling schedule indicates that O_3 likely oxidizes some isoprene to MACR as precursor
542 of 2-MG at BHM. The weak correlation ($r^2 = 0.16$, $n = 75$) between O_3 and 2-methyltetrols early
543 in the day as well as the better correlation ($r^2 = 0.34$, $n = 15$) later in the day (intensive 3, 4-7 PM
544 local time) are consistent with recent laboratory studies demonstrating that 2-methyltetrols can be
545 formed via isoprene ozonolysis in the presence of acidified sulfate aerosol (Riva et al., 2015).

546 Although urban O_3 and nighttime $\text{P}[\text{NO}_3]$ may have a role in local formation of
547 MAE/HMML- and IEPOX-derived SOA tracers at BHM, this does not appear to explain the
548 majority of the SOA tracers, since no significant day-night variation of the entire group of tracers
549 was observed during the campaign. The majority of IEPOX-derived SOA was likely formed when
550 isoprene SOA precursors (IEPOX) were generated upwind and transported to the BHM site. Wind



551 directions during the campaign are consistent with long-range transport of isoprene SOA
552 precursors from southwest of the site, which is covered by forested areas. The absence of a
553 correlation of aerosol acidity with MAE/HMML- and IEPOX-derived SOA tracers indicates that
554 acidity is not the limiting variable that controls formation of these compounds. However, the lack
555 of correlation between SOA tracers and acidity may stem from nearly invariant aerosol acidity
556 throughout the campaign. Hence, despite laboratory studies demonstrating that aerosol acidity can
557 enhance isoprene SOA formation (Surratt et al., 2007; Surratt et al., 2010; Lin et al., 2012), the
558 effect may not be significant in the southeastern U.S. during the summer months due to the constant
559 acidity of aerosols. Future work should examine how well current models can predict the isoprene
560 SOA levels observed during this study, especially since urban emissions are directly present.
561 Furthermore, explicit models are now available to predict the isoprene SOA tracers measured here
562 (McNeill et al., 2012; Pye et al., 2013), which will allow the modeling community to test the
563 current parameterizations that are used to capture the enhancing effect of anthropogenic pollutants
564 on isoprene-derived SOA formation. In addition, the significant correlations of isoprene-derived
565 SOA tracers with P[NO₃] observed during this study indicate a need to better understand nighttime
566 chemistry of isoprene. Lastly, although O₃ appears to have an enhancing effect on isoprene-
567 derived SOA tracers, the intermediates are unknown. Hydroperoxides suggested by Riva et al.
568 (2015) may be key, but chamber experiments with authentic precursors are needed to test this
569 hypothesis.



570 **Acknowledgements**

571 This work was funded by the U.S. Environmental Protection Agency (EPA) through grant number
572 835404. The contents of this publication are solely the responsibility of the authors and do not
573 necessarily represent the official views of the U.S. EPA. Further, the U.S. EPA does not endorse
574 the purchase of any commercial products or services mentioned in the publication. The authors
575 would also like to thank the Electric Power Research Institute (EPRI) for their support. This study
576 was supported in part by the National Oceanic and Atmospheric Administration (NOAA) Climate
577 Program Office's AC4 program, award number NA13OAR4310064. The authors thank the
578 Camille and Henry Dreyfus Postdoctoral Fellowship Program in Environmental Chemistry for
579 their financial support. The authors thank Louisa Emmons and Christoph Knote for their assistance
580 with chemical forecasts made available during the SOAS campaign. We would like to thank
581 Annmarie Carlton, Joost deGouw, Jose Jimenez, and Allen Goldstein for helping to organize the
582 SOAS campaign and coordinating communication between ground sites. UPLC/ESI-HR-Q-
583 TOFMS analyses were conducted in the UNC-CH Biomarker Mass Facility located within the
584 Department of Environmental Sciences and Engineering, which is a part of the UNC-CH Center
585 for Environmental Health and Susceptibility supported by National Institute for Environmental
586 Health Sciences (NIEHS), grant number 5P20-ES10126. WSOC measurements at the University
587 of Iowa were supported through EPA STAR grant 8354101. The authors thank Theran Riedel for
588 useful discussions. We also thank SCG Chemicals Co., Ltd., Siam Cement Group, Thailand, for
589 the full support for W. Rattanavaraha attending UNC, Chapel Hill.

590

591

592 **References**

- 593 Birch, M. E., and Cary, R. A.: Elemental carbon-based method for occupational monitoring of
594 particulate diesel exhaust: methodology and exposure issues, *Analyst*, 121, 1183-1190,
595 1996.
- 596 Blanchard, C. L., Hidy, G. M., Shaw, S., Baumann, K., and Edgerton, E. S.: Effects of emission
597 reductions on organic aerosol in the southeastern United States, *Atmos. Chem. Phys.*
598 *Discuss.*, 15, 17051-17092, doi:10.5194/acpd-15-17051-2015, 2015.
- 599 Boucher, O., Randall, D., Artaxo, P., Bretherton, C., Feingold, G., Forster, P., Kerminen, V.-M.,
600 Kondo, Y., Liao, H., and Lohmann, U.: Clouds and aerosols, in: *Climate change 2013:*
601 *the physical science basis. Contribution of Working Group I to the Fifth Assessment*
602 *Report of the Intergovernmental Panel on Climate Change*, Cambridge University Press,
603 571-657, 2013.
- 604 Budisulistiorini, S., Li, X., Bairai, S., Renfro, J., Liu, Y., Liu, Y., McKinney, K., Martin, S.,
605 McNeill, V., and Pye, H.: Examining the effects of anthropogenic emissions on isoprene-
606 derived secondary organic aerosol formation during the 2013 Southern Oxidant and
607 Aerosol Study (SOAS) at the Look Rock, Tennessee, ground site, *Atmospheric Chemistry*
608 *and Physics Discussions*, 15, 7365-7417, 2015.
- 609 Budisulistiorini, S. H., Canagaratna, M. R., Croteau, P. L., Marth, W. J., Baumann, K., Edgerton,
610 E. S., Shaw, S. L., Knipping, E. M., Worsnop, D. R., and Jayne, J. T.: Real-time
611 continuous characterization of secondary organic aerosol derived from isoprene
612 epoxydiols in downtown Atlanta, Georgia, using the Aerodyne Aerosol Chemical
613 Speciation Monitor, *Environ. Sci. Technol.*, 47, 5686-5694, 2013.
- 614 Carlton, A., Wiedinmyer, C., and Kroll, J.: A review of Secondary Organic Aerosol (SOA)
615 formation from isoprene, *Atmospheric Chemistry and Physics*, 9, 4987-5005, 2009.
- 616 Carlton, A. G., Bhawe, P. V., Napelenok, S. L., Edney, E. O., Sarwar, G., Pinder, R. W., Pouliot,
617 G. A., and Houyoux, M.: Model representation of secondary organic aerosol in CMAQv4.
618 7, *Environ. Sci. Technol.*, 44, 8553-8560, 2010a.
- 619 Carlton, A. G., Pinder, R. W., Bhawe, P. V., and Pouliot, G. A.: To what extent can biogenic SOA
620 be controlled?, *Environ. Sci. Technol.*, 44, 3376-3380, 2010b.



- 621 Chan, A., Chan, M., Surratt, J., Chhabra, P., Loza, C., Crouse, J., Yee, L., Flagan, R., Wennberg,
622 P., and Seinfeld, J.: Role of aldehyde chemistry and NO_x concentrations in secondary
623 organic aerosol formation, *Atmospheric Chemistry and Physics*, 10, 7169-7188, 2010.
- 624 Claeys, M., Graham, B., Vas, G., Wang, W., Vermeylen, R., Pashynska, V., Cafmeyer, J., Guyon,
625 P., Andreae, M. O., and Artaxo, P.: Formation of secondary organic aerosols through
626 photooxidation of isoprene, *Science*, 303, 1173-1176, 2004.
- 627 Ding, X., Zheng, M., Yu, L., Zhang, X., Weber, R. J., Yan, B., Russell, A. G., Edgerton, E. S., and
628 Wang, X.: Spatial and seasonal trends in biogenic secondary organic aerosol tracers and
629 water-soluble organic carbon in the southeastern United States, *Environ. Sci. Technol.*,
630 42, 5171-5176, 2008.
- 631 Edgerton, E. S., Hartsell, B. E., Saylor, R. D., Jansen, J. J., Hansen, D. A., and Hidy, G. M.: The
632 Southeastern Aerosol Research and Characterization Study, part 3: Continuous
633 measurements of fine particulate matter mass and composition, *Journal of the Air &
634 Waste Management Association*, 56, 1325-1341, 2006.
- 635 Edney, E. O., Kleindienst, T. E., Jaoui, M., Lewandowski, M., Offenberg, J. H., Wang, W., and
636 Claeys, M.: Formation of 2-methyl tetrols and 2-methylglyceric acid in secondary organic
637 aerosol from laboratory irradiated isoprene/NO_x/SO₂/air mixtures and their detection in
638 ambient PM_{2.5} samples collected in the eastern United States, *Atmospheric Environment*,
639 39, 5281-5289, <http://dx.doi.org/10.1016/j.atmosenv.2005.05.031>, 2005.
- 640 El-Zanan, H. S., Zielinska, B., Mazzoleni, L. R., and Hansen, D. A.: Analytical determination of
641 the aerosol organic mass-to-organic carbon ratio, *Journal of the Air & Waste Management
642 Association*, 59, 58-69, 2009.
- 643 Emmons, L. K., Walters, S., Hess, P. G., Lamarque, J. F., Pfister, G. G., Fillmore, D., Granier, C.,
644 Guenther, A., Kinnison, D., Laepple, T., Orlando, J., Tie, X., Tyndall, G., Wiedinmyer,
645 C., Baughcum, S. L., and Kloster, S.: Description and evaluation of the Model for Ozone
646 and Related chemical Tracers, version 4 (MOZART-4), *Geosci. Model Dev.*, 3, 43-67,
647 10.5194/gmd-3-43-2010, 2010.
- 648 Foley, K., Roselle, S., Appel, K., Bhave, P., Pleim, J., Otte, T., Mathur, R., Sarwar, G., Young, J.,
649 and Gilliam, R.: Incremental testing of the Community Multiscale Air Quality (CMAQ)
650 modeling system version 4.7, *Geoscientific Model Development*, 3, 205-226, 2010.



- 651 Fountoukis, C., and Nenes, A.: ISORROPIA II: a computationally efficient thermodynamic
652 equilibrium model for K^+ – Ca^{2+} – Mg^{2+} – NH_4^+ – Na^+ – SO_4^{2-} – NO_3^- – Cl^- – H_2O
653 aerosols, *Atmospheric Chemistry and Physics*, 7, 4639-4659, 2007.
- 654 Fountoukis, C., Nenes, A., Sullivan, A., Weber, R., Reken, T. V., Fischer, M., Matias, E., Moya,
655 M., Farmer, D., and Cohen, R.: Thermodynamic characterization of Mexico City aerosol
656 during MILAGRO 2006, *Atmospheric Chemistry and Physics*, 9, 2141-2156, 2009.
- 657 Galloway, M. M., Chhabra, P. S., Chan, A. W. H., Surratt, J. D., Flagan, R. C., Seinfeld, J. H., and
658 Keutsch, F. N.: Glyoxal uptake on ammonium sulphate seed aerosol: reaction products
659 and reversibility of uptake under dark and irradiated conditions, *Atmos. Chem. Phys.*, 9,
660 3331-3345, 10.5194/acp-9-3331-2009, 2009.
- 661 Graham, R. A., and Johnston, H. S.: The photochemistry of the nitrate radical and the kinetics of
662 the nitrogen pentoxide-ozone system, *The Journal of Physical Chemistry*, 82, 254-268,
663 1978.
- 664 Guenther, A. B., Jiang, X., Heald, C. L., Sakulyanontvittaya, T., Duhl, T., Emmons, L. K., and
665 Wang, X.: The Model of Emissions of Gases and Aerosols from Nature version 2.1
666 (MEGAN2.1): an extended and updated framework for modeling biogenic emissions,
667 *Geosci Model Dev*, 5, 1471-1492, 10.5194/gmd-5-1471-2012, 2012.
- 668 Grieshop, A., P., Logue, J., M., Donahue, J., M., and Robinson, A., L.: Laboratory investigation
669 of photochemical oxidation of organic aerosol from wood fires 1 : measurement and
670 simulation of organic aerosol evolution, *Atmos. Chem. Phys.*, 9, 1263-1277, 2009.
- 671 Hallquist, M., Wenger, J. C., Baltensperger, U., Rudich, Y., Simpson, D., Claeys, M., Dommen,
672 J., Donahue, N. M., George, C., Goldstein, A. H., Hamilton, J. F., Herrmann, H.,
673 Hoffmann, T., Iinuma, Y., Jang, M., Jenkin, M. E., Jimenez, J. L., Kiendler-Scharr, A.,
674 Maenhaut, W., McFiggans, G., Mentel, T. F., Monod, A., Prévôt, A. S. H., Seinfeld, J.
675 H., Surratt, J. D., Szmigielski, R., and Wildt, J.: The formation, properties and impact of
676 secondary organic aerosol: current and emerging issues, *Atmos. Chem. Phys.*, 9, 5155-
677 5236, 10.5194/acp-9-5155-2009, 2009.
- 678 Hansen, D. A., Edgerton, E. S., Hartsell, B. E., Jansen, J. J., Kandasamy, N., Hidy, G. M., and
679 Blanchard, C. L.: The Southeastern aerosol research and characterization study: part 1—
680 overview, *Journal of the Air & Waste Management Association*, 53, 1460-1471, 2003.



- 681 Henze, D. K., Seinfeld, J. H., and Shindell, D. T.: Inverse modeling and mapping US air quality
682 influences of inorganic PM 2.5 precursor emissions using the adjoint of GEOS-Chem,
683 Atmospheric Chemistry and Physics, 9, 5877-5903, 2009.
- 684 Herron, J. T., and Huie, R. E.: Rate constants for the reactions of ozone with ethene and propene,
685 from 235.0 to 362.0. deg. K, The Journal of Physical Chemistry, 78, 2085-2088, 1974.
- 686 Hu, W., Campuzano-Jost, P., Palm, B., Day, D., Ortega, A., Hayes, P., Krechmer, J., Chen, Q.,
687 Kuwata, M., and Liu, Y.: Characterization of a real-time tracer for Isoprene Epoxydiols-
688 derived Secondary Organic Aerosol (IEPOX-SOA) from aerosol mass spectromete-
689 r measurements, Atmospheric Chemistry and Physics Discussions, 15, 11223-11276, 2015.
- 690 Kamens, R., Gery, M., Jeffries, H., Jackson, M., and Cole, E.: Ozone-isoprene reactions: product
691 formation and aerosol potential, Int. J. Chem. Kinet., 14, 955-975, 1982.
- 692 Kanakidou, M., Seinfeld, J. H., Pandis, S. N., Barnes, I., Dentener, F. J., Facchini, M. C., Van
693 Dingenen, R., Ervens, B., Nenes, A., Nielsen, C. J., Swietlicki, E., Putaud, J. P.,
694 Balkanski, Y., Fuzzi, S., Horth, J., Moortgat, G. K., Winterhalter, R., Myhre, C. E. L.,
695 Tsigaridis, K., Vignati, E., Stephanou, E. G., and Wilson, J.: Organic aerosol and global
696 climate modelling: a review, Atmos. Chem. Phys., 5, 1053-1123, 10.5194/acp-5-1053-
697 2005, 2005.
- 698 Karambelas, A., Pye, H. O., Budisulistiorini, S. H., Surratt, J. D., and Pinder, R. W.: Contribution
699 of isoprene epoxydiol to urban organic aerosol: evidence from modeling and
700 measurements, Environmental Science & Technology Letters, 1, 278-283, 2014.
- 701 Kroll, J. H., Ng, N. L., Murphy, S. M., Flagan, R. C., and Seinfeld, J. H.: Secondary organic aerosol
702 formation from isoprene photooxidation under high-NO_x conditions, Geophysical
703 Research Letters, 32, 2005.
- 704 Kroll, J. H., Ng, N. L., Murphy, S. M., Flagan, R. C., and Seinfeld, J. H.: Secondary Organic
705 Aerosol Formation from Isoprene Photooxidation, Environ. Sci. Technol., 40, 1869-1877,
706 10.1021/es0524301, 2006.
- 707 Liao, J., Froyd, K. D., Murphy, D. M., Keutsch, F. N., Yu, G., Wennberg, P. O., St Clair, J. M.,
708 Crouse, J. D., Wisthaler, A., and Mikoviny, T.: Airborne measurements of
709 organosulfates over the continental US, Journal of Geophysical Research: Atmospheres,
710 120, 2990-3005, 2015.



- 711 Lin, Y.-H., Zhang, Z., Docherty, K. S., Zhang, H., Budisulistiorini, S. H., Rubitschun, C. L., Shaw,
712 S. L., Knipping, E. M., Edgerton, E. S., and Kleindienst, T. E.: Isoprene epoxydiols as
713 precursors to secondary organic aerosol formation: acid-catalyzed reactive uptake studies
714 with authentic compounds, *Environ. Sci. Technol.*, 46, 250-258, 2012.
- 715 Lin, Y.-H., Zhang, H., Pye, H. O., Zhang, Z., Marth, W. J., Park, S., Arashiro, M., Cui, T.,
716 Budisulistiorini, S. H., and Sexton, K. G.: Epoxide as a precursor to secondary organic
717 aerosol formation from isoprene photooxidation in the presence of nitrogen oxides,
718 *Proceedings of the National Academy of Sciences*, 110, 6718-6723, 2013a.
- 719 Lin, Y. H., Knipping, E. M., Edgerton, E. S., Shaw, S. L., and Surratt, J. D.: Investigating the
720 influences of SO₂ and NH₃ levels on isoprene-derived secondary organic aerosol
721 formation using conditional sampling approaches, *Atmos. Chem. Phys.*, 13, 8457-8470,
722 10.5194/acp-13-8457-2013, 2013b.
- 723 Lin, Y.-H., Budisulistiorini, S. H., Chu, K., Siejack, R. A., Zhang, H., Riva, M., Zhang, Z., Gold,
724 A., Kautzman, K. E., and Surratt, J. D.: Light-absorbing oligomer formation in secondary
725 organic aerosol from reactive uptake of isoprene epoxydiols, *Environ. Sci. Technol.*, 48,
726 12012-12021, 2014.
- 727 McNeill, V. F., Woo, J. L., Kim, D. D., Schwier, A. N., Wannell, N. J., Sumner, A. J., & Barakat,
728 J. M.: Aqueous-phase secondary organic aerosol and organosulfate formation in
729 atmospheric aerosols: a modeling study, *Environ. Sci. Technol.*, 46(15), 8075-8081,
730 2012.
- 731 Nenes, A., Pandis, S. N., and Pilinis, C.: ISORROPIA: A new thermodynamic equilibrium model
732 for multiphase multicomponent inorganic aerosols, *Aquatic geochemistry*, 4, 123-152,
733 1998.
- 734 Ng, N., Kwan, A., Surratt, J., Chan, A., Chhabra, P., Sorooshian, A., Pye, H., Crouse, J.,
735 Wennberg, P., and Flagan, R.: Secondary organic aerosol (SOA) formation from reaction
736 of isoprene with nitrate radicals (NO₃), *Atmospheric Chemistry and Physics*, 8, 4117-
737 4140, 2008.
- 738 Nguyen, T., Coggon, M., Bates, K., Zhang, X., Schwantes, R., Schilling, K., Loza, C., Flagan, R.,
739 Wennberg, P., and Seinfeld, J.: Organic aerosol formation from the reactive uptake of
740 isoprene epoxydiols (IEPOX) onto non-acidified inorganic seeds, *Atmospheric
741 Chemistry and Physics*, 14, 3497-3510, 2014.



- 742 Nguyen, T. B., Bates, K. H., Crouse, J. D., Schwantes, R. H., Zhang, X., Kjaergaard, H. G.,
743 Surratt, J. D., Lin, P., Laskin, A., and Seinfeld, J. H.: Mechanism of the hydroxyl radical
744 oxidation of methacryloyl peroxyxynitrate (MPAN) and its pathway toward secondary
745 organic aerosol formation in the atmosphere, *PCCP*, 17, 17914-17926, 2015.
- 746 Nozière, B., Kalberer, M., Claeys, M., Allan, J., D'Anna, B., Decesari, S., Finessi, E., Glasius,
747 M., Grgić, I., and Hamilton, J. F.: The Molecular Identification of Organic Compounds
748 in the Atmosphere: State of the Art and Challenges, *Chem. Rev.*, 10.1021/cr5003485,
749 2015.
- 750 Pope, C. A., and Dockery, D. W.: Health Effects of Fine Particulate Air Pollution: Lines that
751 Connect, *Journal of the Air & Waste Management Association*, 56, 709-742,
752 10.1080/10473289.2006.10464485, 2006.
- 753 Pye, H. O., Pinder, R. W., Piletic, I. R., Xie, Y., Capps, S. L., Lin, Y.-H., Surratt, J. D., Zhang, Z.,
754 Gold, A., and Luecken, D. J.: Epoxide pathways improve model predictions of isoprene
755 markers and reveal key role of acidity in aerosol formation, *Environ. Sci. Technol.*, 47,
756 11056-11064, 2013.
- 757 Riedel, T. P., Lin, Y.-H., Budisulistiorini, S. H., Gaston, C. J., Thornton, J. A., Zhang, Z., Vizuete,
758 W., Gold, A., and Surratt, J. D.: Heterogeneous reactions of isoprene-derived epoxides:
759 reaction probabilities and molar secondary organic aerosol yield estimates,
760 *Environmental Science & Technology Letters*, 2, 38-42, 2015.
- 761 Riva, M., Budisulistiorini, S. H., Zhang, Z., Gold, A., and Surratt, J. D.: Chemical characterization
762 of secondary organic aerosol constituents from isoprene ozonolysis in the presence of
763 acidic aerosol, *Atmospheric Environment*, 2015.
- 764 Ruthenburg, T. C., Perlin, P. C., Liu, V., McDade, C. E., and Dillner, A. M.: Determination of
765 organic matter and organic matter to organic carbon ratios by infrared spectroscopy with
766 application to selected sites in the IMPROVE network, *Atmospheric Environment*, 86,
767 47-57, 2014.
- 768 Schwantes, R. H., Teng, A. P., Nguyen, T. B., Coggon, M. M., Crouse, J. D., St. Clair, J. M.,
769 Zhang, X., Schilling, K. A., Seinfeld, J. H., and Wennberg, P. O.: Isoprene NO₃ Oxidation
770 Products from the RO₂+ HO₂ Pathway, *The Journal of Physical Chemistry A*, 2015.



- 771 Simon, H., Bhawe, P. V., Swall, J. L., Frank, N. H., and Malm, W. C.: Determining the spatial and
772 seasonal variability in OM/OC ratios across the US using multiple regression, *Atmos.*
773 *Chem. Phys.*, 11, 2933-2949, 10.5194/acp-11-2933-2011, 2011.
- 774 Starn, T., Shepson, P., Bertman, S., Riemer, D., Zika, R., and Olszyna, K.: Nighttime isoprene
775 chemistry at an urban-impacted forest site, *Journal of Geophysical Research:*
776 *Atmospheres* (1984–2012), 103, 22437-22447, 1998.
- 777 Stohl, A., Forster, C., Frank, A., Seibert, P., and Wotawa, G.: Technical note: The Lagrangian
778 particle dispersion model FLEXPART version 6.2, *Atmos. Chem. Phys.*, 5, 2461-2474,
779 10.5194/acp-5-2461-2005, 2005.
- 780 Surratt, J. D., Murphy, S. M., Kroll, J. H., Ng, N. L., Hildebrandt, L., Sorooshian, A., Szmigielski,
781 R., Vermeylen, R., Maenhaut, W., and Claeys, M.: Chemical composition of secondary
782 organic aerosol formed from the photooxidation of isoprene, *The Journal of Physical*
783 *Chemistry A*, 110, 9665-9690, 2006.
- 784 Surratt, J. D., Kroll, J. H., Kleindienst, T. E., Edney, E. O., Claeys, M., Sorooshian, A., Ng, N. L.,
785 Offenberg, J. H., Lewandowski, M., and Jaoui, M.: Evidence for organosulfates in
786 secondary organic aerosol, *Environ. Sci. Technol.*, 41, 517-527, 2007a.
- 787 Surratt, J. D., Lewandowski, M., Offenberg, J. H., Jaoui, M., Kleindienst, T. E., Edney, E. O., and
788 Seinfeld, J. H.: Effect of acidity on secondary organic aerosol formation from isoprene,
789 *Environ. Sci. Technol.*, 41, 5363-5369, 2007b.
- 790 Surratt, J. D., Chan, A. W., Eddingsaas, N. C., Chan, M., Loza, C. L., Kwan, A. J., Hersey, S. P.,
791 Flagan, R. C., Wennberg, P. O., and Seinfeld, J. H.: Reactive intermediates revealed in
792 secondary organic aerosol formation from isoprene, *Proceedings of the National*
793 *Academy of Sciences*, 107, 6640-6645, 2010.
- 794 Tanner, R. L., Bairai, S. T., Olszyna, K. J., Valente, M. L., and Valente, R. J.: Diurnal patterns in
795 PM 2.5 mass and composition at a background, complex terrain site, *Atmospheric*
796 *Environment*, 39, 3865-3875, 2005.
- 797 Wang, W., Kourtchev, I., Graham, B., Cafmeyer, J., Maenhaut, W., and Claeys, M.:
798 Characterization of oxygenated derivatives of isoprene related to 2-methyltetrols in
799 Amazonian aerosols using trimethylsilylation and gas chromatography/ion trap mass
800 spectrometry, *Rapid Commun. Mass Spectrom.*, 19, 1343-1351, 2005.



- 801 Xu, L., Guo, H., Boyd, C. M., Klein, M., Bougiatioti, A., Cerully, K. M., Hite, J. R., Isaacman-
802 VanWertz, G., Kreisberg, N. M., and Knote, C.: Effects of anthropogenic emissions on
803 aerosol formation from isoprene and monoterpenes in the southeastern United States,
804 Proceedings of the National Academy of Sciences, 112, 37-42, 2015.
- 805 Zhang, Z., Lin, Y.-H., Zhang, H., Surratt, J., Ball, L., and Gold, A.: Technical Note: Synthesis of
806 isoprene atmospheric oxidation products: isomeric epoxydiols and the rearrangement
807 products cis-and trans-3-methyl-3, 4-dihydroxytetrahydrofuran, Atmospheric Chemistry
808 and Physics, 12, 8529-8535, 2012.
- 809



810 **Table 1.** Sampling schedule during SOAS at the BHM ground site.

No. of samples/ day	Sampling schedule	Dates
2 (regular)	Day: 8 am – 7 pm Night: 8 pm – 7 am next day	June 1 – June 9 June 13, June 17 – June 28, July 2- July 9, July 15
4 (intensive)	Intensive 1: 8 am – 12 pm, Intensive 2: 1 pm – 3 pm, Intensive 3: 4 pm – 7 pm, Intensive 4: 8 pm – 7 am next day	June 10 – June 12, June 14 – June 16, June 29 – June 30, July 1, July 9 – July 14

811

812 **Table 2.** Summary of collocated measurements of meteorological variables, gaseous species, and
 813 PM_{2.5} constituents.

814

Category	Condition	Average	SD	Minimum	Maximum
Meteorology	Rainfall (in)	0.1	0.2	0.0	1.4
	Temp (°C)	26.4	3.0	20.5	32.7
	RH (%)	71.5	15.0	36.9	96.1
	BP (mbar)	994.2	3.9	984.2	1002.4
	SR (W m ⁻²)	303.7	274.5	7.0	885.0
Trace gas (ppbv)	O ₃	31.1	14.8	8.3	62.2
	CO	208.7	72.0	99.6	422.9
	SO ₂	0.9	0.8	0.1	3.7
	NO	1.3	1.2	0.1	7.0
	NO ₂	6.6	5.1	1.0	22.7
	NO _x	7.8	6.0	1.3	29.7
	NO _y	9.1	5.8	2.2	30.4
	HNO ₃	0.3	0.2	0.1	1.0
	NH ₃	1.9	0.8	0.7	4.0
PM _{2.5} (μg m ⁻³)	OC	7.2	3.2	1.4	14.9
	EC	0.6	0.5	0.1	2.7
	WSOC	4.0	1.8	0.5	7.5
	SO ₄ ²⁻	2.0	0.9	0.4	4.9
	NO ₃ ⁻	0.1	0.1	0.0	0.8
	NH ₄ ⁺	0.7	0.3	0.2	1.2
	Aerosol pH	1.8	0.1	1.6	1.9


 815 **Table 3.** Summary of isoprene-derived SOA tracers measured by GC/EI-MS and UPLC/ESI-HR-QTOFMS

SOA tracers	<i>m/z</i>	Frequency of detection (%) ^a	Max concentration (ng/m ³)	Mean concentration (ng/m ³)	Isoprene SOA Mass fraction (%) ^b	% of total OM ^c
Measured by GC/EI-MS						
2-methylerythritol ^d	219	99.2	1048.9	269.0	33.8	2.7
2-methylthreitol ^d	219	100.0	388.9	107.3	13.5	1.1
(E)-2-methylbut-3-ene-1,2,4-triol ^e	231	96.7	878.9	112.7	14.2	1.1
(Z)-2-methylbut-3-ene-1,2,4-triol ^e	231	95.8	287.8	38.9	4.9	0.4
2-methylbut-3-ene-1,2,3-triol ^e	231	94.2	503.3	28.9	3.6	0.3
2-methylglyceric acid ^d	219	93.3	35.0	10.8	1.4	0.1
<i>cis</i> -3-MeTHF-3,4-diol ^d	262	22.5	98.9	6.9	0.9	0.1
<i>trans</i> -3-MeTHF-3,4-diol ^d	262	10.0	137.6	8.6	1.1	0.1
IEPOX-derived dimer ^e	333	10.0	2.2	0.0	0.0	0.0
Levoglucofan ^d	204	100.0	922.6	98.7	-	1.0
Measured by UPLC/ESI-HR-QTOFMS						
IEPOX-derived OSs						
C ₅ H ₁₁ O ₇ S ^{-d}	215	100.0	864.9	164.5	20.7	1.6
C ₁₀ H ₂₁ O ₁₀ S ^{-f}	333	1.7	0.3	0.0	0.0	0.0
MAE-derived OS ^d						
C ₄ H ₇ O ₇ S ⁻	199	100.0	35.7	7.2	1.9	0.1
GA sulfate ^d						
C ₂ H ₃ O ₆ S ⁻	155	100.0	75.2	26.2	3.3	0.3
Methylglyoxal-derived OS ^g						
C ₃ H ₅ O ₆ S ⁻	169	97.5	10.5	2.7	0.3	0.0
Isoprene-derived OSs ^g						
C ₅ H ₇ O ₇ S ⁻	211	97.5	5.2	1.4	0.2	0.0
C ₅ H ₁₀ NO ₉ S ⁻	260	90.0	3.9	0.3	0.0	0.0
C ₅ H ₉ N ₂ O ₁₁ S ⁻	305	5.0	3.3	2.9	0.4	0.0
Hydroxyacetone-derived OS ^g						
C ₂ H ₃ O ₅ S ⁻	139	30.8	2.6	0.2	0.0	0.0

^a Total filters = 120

^b Mass fraction is the contribution of each species among total known isoprene-derived SOA mass detected by GC/EI MS and UPLC/ESI-HR-QTOFMS

^c OM/OC = 1.6

^d OA tracers quantified by authentic standards

^e SOA tracers quantified by 2-methyltetrols as a surrogate standard

^f SOA tracer quantified by IEPOX-derived OS (*m/z* 215) as a surrogate standard

^g SOA tracers quantified by propyl sulfate as a surrogate standard



822 **Table 4.** Overall correlation (r^2) of isoprene-derived SOA tracers and collocated measurements at
 823 BHM during 2013 SOAS campaign.

SOA tracers	CO	O ₃	NO _x	NO _y	SO ₂	NH ₃	SO ₄	NO ₃	NH ₄	OC	WSOC	pH
MAE/HMML-derived SOA tracers	0.07	0.26	0.00	0.01	0.06	0.11	0.33	0.01	0.18	0.47	0.20	0.00
2-methylglyceric acid	0.01	0.26	0.01	0.00	0.01	0.07	0.10	0.00	0.06	0.19	0.02	0.00
MAE-derived OS	0.10	0.14	0.00	0.02	0.07	0.09	0.38	0.01	0.18	0.32	0.23	0.01
IEPOX-derived SOA tracers	0.04	0.05	0.00	0.01	0.05	0.01	0.36	0.00	0.21	0.24	0.12	0.00
2-methylerythritol	0.00	0.16	0.03	0.02	0.01	0.00	0.30	0.02	0.18	0.18	0.19	0.00
2-methylthreitol	0.00	0.13	0.02	0.03	0.02	0.00	0.20	0.01	0.16	0.17	0.15	0.00
(E)-2-methylbut-3-ene-1,2,4-triol	0.07	0.00	0.02	0.01	0.07	0.00	0.15	0.00	0.19	0.11	0.04	0.00
(Z)-2-methylbut-3-ene-1,2,4-triol	0.04	0.00	0.00	0.00	0.06	0.00	0.28	0.00	0.20	0.04	0.00	0.00
2-methylbut-3-ene-1,2,3-triol	0.02	0.00	0.03	0.00	0.00	0.02	0.32	0.01	0.03	0.17	0.04	0.00
IEPOX-derived OS	0.02	0.14	0.03	0.00	0.00	0.00	0.27	0.00	0.16	0.29	0.29	0.00
IEPOX dimer	0.00	0.00	0.00	0.00	0.00	0.00	0.00	0.00	0.00	0.00	0.00	0.00
Other isoprene SOA tracers												
GA sulfate												
C ₂ H ₃ O ₆ S ⁻	0.30	0.23	0.01	0.00	0.08	0.09	0.27	0.00	0.19	0.38	0.18	0.00
Methylglyoxal-derived OS												
C ₃ H ₅ O ₆ S ⁻	0.14	0.04	0.02	0.03	0.03	0.07	0.31	0.02	0.25	0.21	0.24	0.00
Isoprene-derived OSs												
C ₅ H ₇ O ₇ S ⁻	0.01	0.23	0.03	0.01	0.00	0.02	0.21	0.00	0.16	0.31	0.13	0.00
C ₅ H ₁₀ NO ₆ S ⁻	0.17	0.00	0.12	0.14	0.10	0.14	0.31	0.16	0.23	0.20	0.07	0.00
C ₅ H ₉ N ₂ O ₁₁ S ^{-*}	0.32	0.71	0.66	0.58	0.42	0.02	0.68	0.50	0.42	0.00	0.50	0.00
Hydroxyacetone-derived OS												
C ₂ H ₃ O ₅ S ⁻	0.02	0.10	0.08	0.07	0.05	0.00	0.00	0.03	0.00	0.01	0.01	0.00
Other tracer												
Levogluconan	0.00	0.09	0.02	0.01	0.02	0.00	0.00	0.02	0.00	0.08	0.04	0.01

824 * Found only in 6 of 120 filters

825 The correlations in this table are positive.

826

827

828

829

830

831

832

833



834 **Table 5.** Summary of isoprene-derived SOA tracers from the three SOAS ground sites: BHM,
 835 CTR, and LRK.

836

SOA tracers	Urban		Rural			
	BHM		CTR		LRK	
	Mean (ng m ⁻³)	Average amount detected tracers (%)	Mean (ng m ⁻³)	Average amount detected tracers (%)	Mean (ng m ⁻³)	Average amount detected tracers (%)
MAE/HMML derived SOA						
MAE/HMML-derived OS	7.2	1.1	10.2	1.3	8.2	1.8
2-methylglyceric acid	10.4	1.7	5.1	0.7	7.5	1.6
IEPOX derived SOA						
IEPOX-derived OS	164.5	24.3	207.1	26.8	139.2	30.3
IEPOX-derived dimer OS	0.04	0.00	0.7	0.1	1.1	0.2
2-methylerythritol	266.7	37.9	204.8	26.5	120.7	26.3
2-methylthreitol	107.3	15.8	73.7	9.5	42.4	9.2
(E)-2-methylbut-3-ene-1,2,4-triol	109.0	12.3	137.3	17.8	98.8	21.5
(Z)-2-methylbut-3-ene-1,2,4-triol	37.3	4.1	50.7	6.6	29.1	6.1
2-methylbut-3-ene-1,2,3-triol	23.4	2.5	26.1	3.4	16.5	3.6
trans-3-MeTHF-3,4-diol	8.6	1.0	0.0	0.0	2.7	0.6
cis-3-MeTHF-3,4-diol	6.8	1.0	0.2	0.0	1.7	0.4

837



838

839

840

841

842

843

844

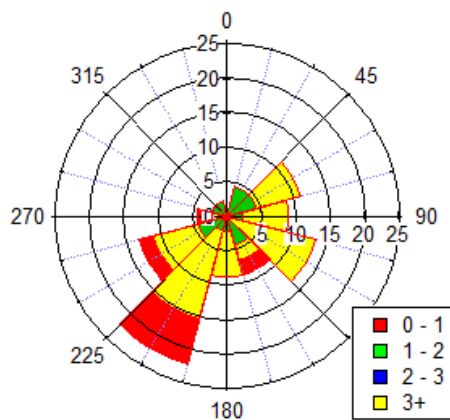
845

846

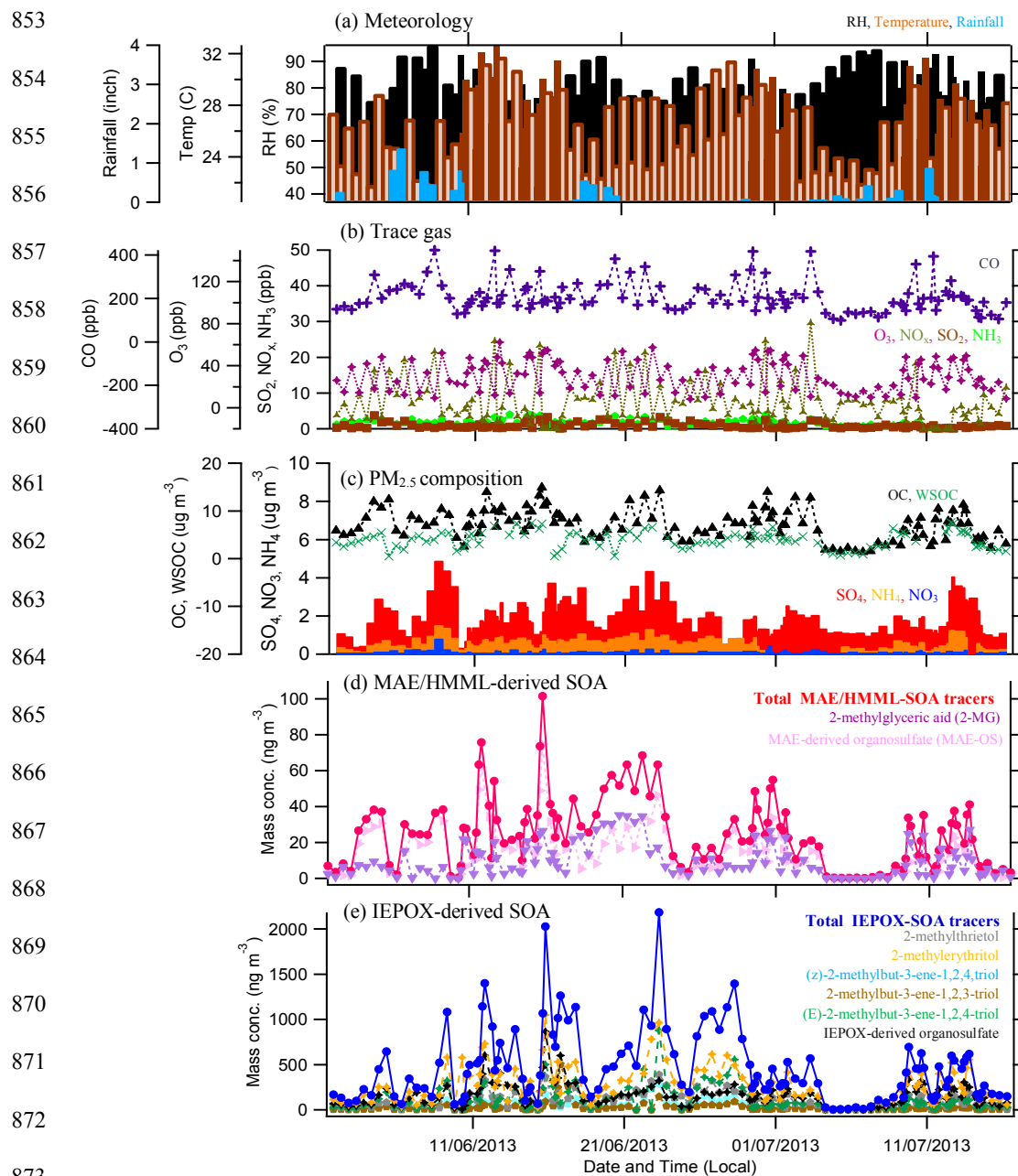
847

848

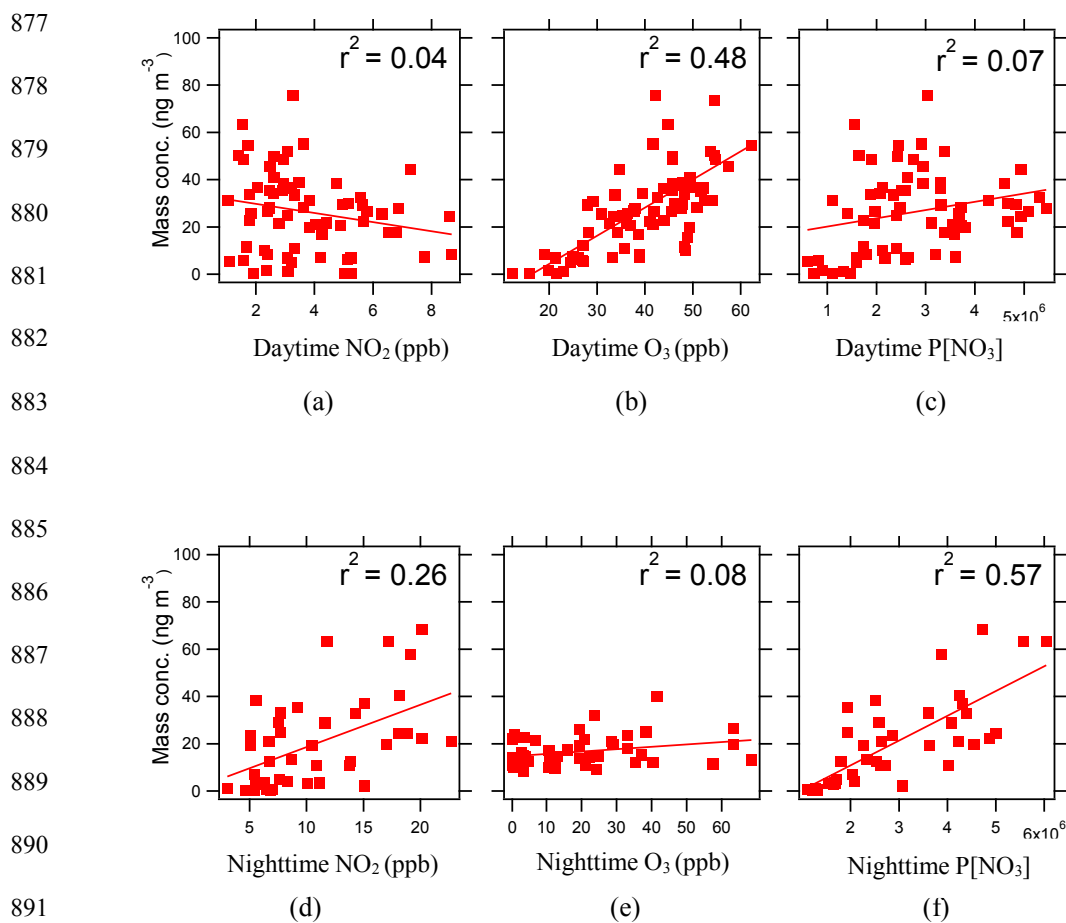
849



850 **Figure 1.** Wind rose illustrating wind direction during the campaign at the BHM site. Bars indicate
851 direction of incoming wind, with 0 degrees set to geographic north. Length of bar size indicates
852 frequency with color segments indicating the wind speed in m s^{-1} .



874 **Figure 2.** Time series of (a) meteorological data, (b) trace gases, (c) PM_{2.5} constituents, (d)
875 MAE/HMML-derived SOA tracers and (e) IEPOX-derived SOA tracers during the 2013 SOAS
876 campaign at the BHM site.



893 **Figure 3.** Correlation of MAE-derived SOA tracers with (a) daytime NO₂, (b) daytime O₃, (c)
894 daytime P[NO₃], (d) nighttime NO₂, (e) nighttime O₃, and (f) nighttime P[NO₃]. Nighttime P[NO₃]
895 correlation suggests that NO₃ radical chemistry could explain some fraction of the MAE/HMML-
896 derived SOA tracer concentrations.

897

898



899

900

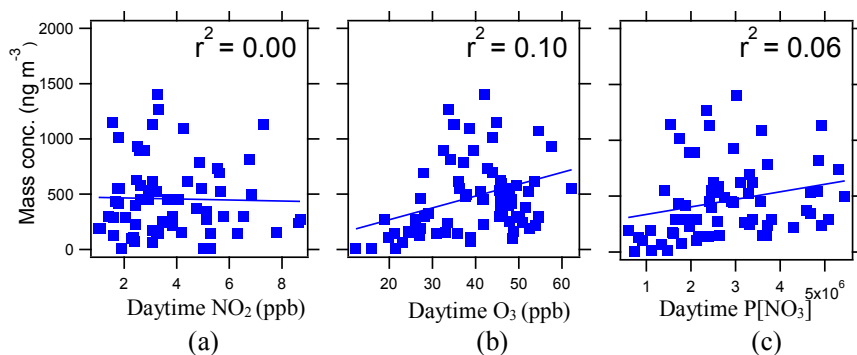
901

902

903

904

905



906

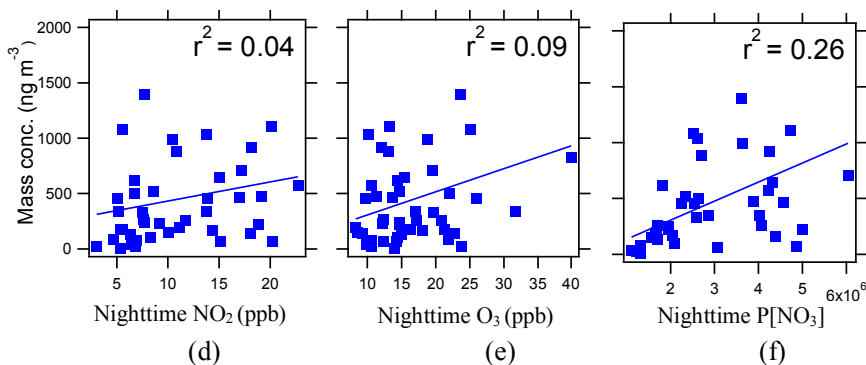
907

908

909

910

911



912

913 **Figure 4.** Correlation of IEPOX-derived SOA tracers with (a) daytime NO₂, (b) daytime O₃, (c)
914 daytime P[NO₃], (d) nighttime NO₂, (e) nighttime O₃, and (f) nighttime P[NO₃]. Nighttime P[NO₃]
915 correlation suggests that NO₃ radical chemistry could explain some fraction of the IEPOX-derived
916 SOA tracer concentrations.